Gain–Bandwidth Properties of a Class of Matched Feedback Amplifiers

DAVID J. AHLGREN, MEMBER, IEEE, AND WALTER H. KU, MEMBER, IEEE

Abstract —**This paper considers the analysis and synthesis of small-signal feedback amplifiers which use shunt feedback around a generic gain block. The analysis presented leads to estimates of all network element values and predicts the closed-loop broad-band gain, bandwidth, and quality of match at both ports. The tradeoff of gain for quality of match is made evident by a graphical technique. The paper also describes a synthesis method and two illustrative design examples.**

I. Introduction

MATCHED BROAD-BAND solid-state feedback amplifiers enjoy wide application in communication and instrumentation systems. It has been shown that these amplifiers exhibit gain–bandwidth and noise performance which compares favorably to the performance of the distributed amplifier and the lossy-match amplifier [1]. Analysis of the noise properties of such amplifiers has been presented in [2], and the measured performance of feedback amplifiers using GaAs MESFET's has been described in [1] and in [3]–[15].

In such papers, the analysis of gain and matching has been approximate and limited to the low-frequency case [8], [13], [14]. In contrast, this paper presents a detailed broad-band small-signal analysis of the gain and matching properties of low-pass feedback amplifiers which employ resistive shunt feedback around an active gain block (Fig. 1). The gain block, which may consist of a single active device or a more complex circuit, is modeled by one of two unilateral frequency-dependent equivalent circuits. The analysis treats both the low- and high-frequency properties of the feedback amplifier, leads to estimates of all network element values, and predicts the closed-loop broad-band gain, −3-dB bandwidth, and the quality of input and output matches. Predicted values of network elements serve well as starting values for an optimization step by computer.

The analysis presented here considers only small-signal behavior. Biasing is a problem associated with designing the particular gain block and is not discussed. Still, the analysis is general in that it does not require detailed knowledge of the arrangement of active devices within the gain block, so the gain block may contain FET's or BJT's in several circuit configurations.

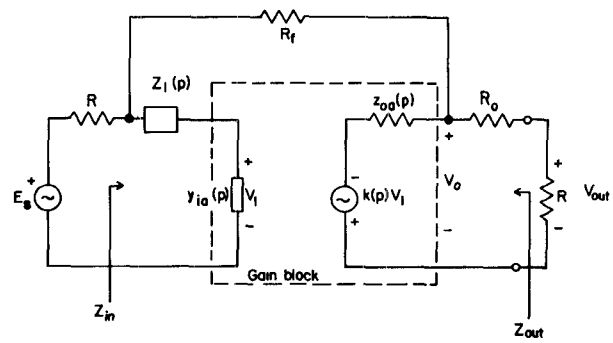

Fig. 1. Basic feedback amplifier.

The paper begins by studying the gain and matching properties of a basic feedback amplifier at low frequencies. The tradeoff of gain and quality of port match is illustrated by a graphical technique, and conditions which lead to simultaneous perfect matches are derived. The paper then presents a broad-banding technique which yields predictions of the closed-loop bandwidth and the quality of high-frequency port matches. Finally, a systematic design procedure and two design examples are presented. The second design example describes a direct-coupled feedback amplifier, suitable for monolithic realization, whose predicted transducer power gain is 7.8 ± 0.2 dB from dc to 7 GHz and predicted −3-dB bandwidth is nearly 9 GHz.

II. The Basic Feedback Amplifier

The basic shunt feedback amplifier shown in Fig. 1 consists of a unilateral gain block, a shunt feedback resistance R_f, a series output resistance R_o, and a series impedance Z_1 which is used to broad-band the amplifier response. The input admittance and the output impedance of the gain block are denoted by $y_{ia}(p)$ and $z_{oa}(p)$, respectively, where $p = \sigma + j\omega$ is the complex frequency variable.

The small-signal equivalent circuit shown in Fig. 2 may be used to calculate the open- and closed-loop transducer voltage gain and input and output immittances of the feedback amplifier. As noted on Fig. 2, we can calculate

Manuscript received July 12, 1986; revised October 23, 1986. This work was supported in part by the Joint Services Electronics Program at Cornell University under AFOSR Contract F49620-81-C-0082 and by an Independent Research Grant from Trinity College.

D. Ahlgren was at Cornell University, Ithaca, NY, on leave from the Department of Engineering and Computer Science, Trinity College, Hartford, CT 06106.

W. H. Ku is with the Department of Electrical Engineering and Computer Sciences, University of California at San Diego, La Jolla, CA 92093.

IEEE Log Number 8612954.

0018-9480/87/0400-0361$01.00 ©1987 IEEE

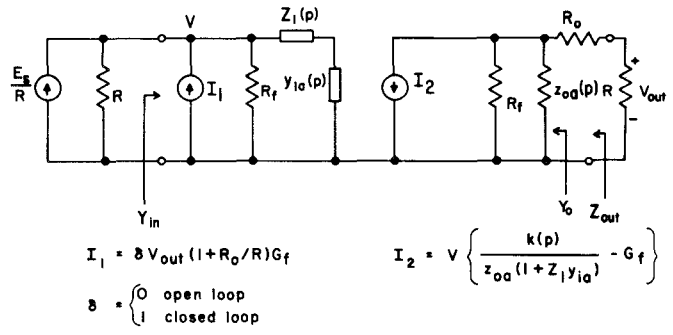

Fig. 2. Basic feedback amplifier equivalent circuit.

the open-loop transducer voltage gain by assigning $\delta = 0$ (δ is defined in Fig. 2), and we can calculate the closed-loop gain by setting $\delta = 1$. By straightforward analysis, we obtain the open-loop transducer voltage gain

$$A_o(p) \doteq \left.\frac{V_{out}(p)}{E_s(p)}\right|_{\delta=0}$$

or

$$A_o(p) = \frac{-k(p)R + RG_f z_{oa}(p)[1+Z_1(p)y_{ia}(p)]}{\{R_o + R + z_{oa}(p)[1+G_f(R_o+R)]\}\{[1+Z_1(p)y_{ia}(p)][1+RG_f] + Ry_{ia}(p)\}} \tag{1}$$

where $k(p)$ is the open-circuit voltage gain of the gain block. For such simple gain blocks as single FET's or two-stage circuits with one high-gain stage and a source follower, $k(p)$ may be approximated by the single-pole function

$$k(p) = \frac{k_o}{1+p\tau_o} \tag{2}$$

where k_o is the open-circuit voltage gain and where $p = -1/\tau_o$ is the dominant pole of $k(p)$. The closed-loop transducer voltage gain is

$$A_f(p) = \frac{A_o(p)}{1-(R_o+R)G_f A_o(p)} \tag{3}$$

and the closed-loop input admittance and the output impedance are

$$Y_{in}(p) = \frac{y_{ia}(p)}{1+Z_1(p)y_{ia}(p)} + \frac{1}{R_f + z_{oa}(p)\|(R_o+R)} \times\left\{1 + \frac{k(p)(R_o+R)}{[z_{oa}(p)+R_o+R][1+Z_1(p)y_{ia}(p)]}\right\} \tag{4}$$

and

$$Z_{out}(p) = R_o + z_{oa}(p)\left\{\frac{[1+RG_f+Ry_{ia}(p)][1+Z_1(p)y_{ia}(p)]}{[1+RG_f+Ry_{ia}(p)][1+Z_1(p)y_{ia}(p)]+k(p)RG_f}\right\}. \tag{5}$$

By using these relationships, we can investigate the trade-off of gain and matching performance of the feedback amplifier.

To evaluate the low-frequency behavior, we assume that $y_{ia}(j0) \ll R^{-1}$, a condition that holds for both FET and BJT input stages. Letting $z_{oa}(j0) = r_{oa}$, we obtain

$$Y_{in}(j0) = \frac{(k_o+1)(R_o+R)+r_{oa}}{(R_f+r_{oa})(R_o+R)+r_{oa}R_f} \tag{6}$$

and

$$Z_{out}(j0) = R_o + r_{oa}\left[\frac{1+RG_f}{1+(k_o+1)RG_f}\right]. \tag{7}$$

For perfect port matches, we set $Y_{in}(j0) = R^{-1}$ in (6) and $Z_{out}(j0) = R$ in (7), obtaining

$$R_f = \frac{(k_o+1)(R_o+R)R - r_{oa}R_o}{r_{oa}+R_o+R} \tag{8}$$

and

$$R_o = R - r_{oa}\left[\frac{1+RG_f}{1+(k_o+1)RG_f}\right]. \tag{9}$$

It follows from (8) and (9) that the input and output ports are simultaneously matched when

$$R_f = Qr_{oa} \tag{10}$$

and when

$$R_o = r_{oa}\left\{\frac{Q\left[1+\frac{R}{r_{oa}}\right] - (k_o+1)\left[\frac{R}{r_{oa}}\right]^2}{(k_o+1)\frac{R}{r_{oa}} - Q - 1}\right\} \tag{11}$$

where

$$Q \doteq \left\{1+4\left(\frac{R}{r_{oa}}\right)^2\left[\frac{k_o+1}{k_o+2}\right]^2\right\}^{1/2} - 1. \tag{12}$$

In typical amplifiers, conditions (10) and (11) lead to low closed-loop gain, so the quality of match must be sacrificed to achieve acceptable gain. In particular, the series output resistance R_o decreases gain and should be included only when the output match must be carefully controlled. It is significant to note that (10) and (11) demonstrate that by matching both ports perfectly we

exhaust all available degrees of freedom. Furthermore, given $0 < R_o < R$, we may derive from (3) and (4) the following bound on the return ratio:

$$1 - \frac{(R_o + R)A_o(j0)}{R_f} < 1 + \frac{k_o}{k_o + 1 + \dfrac{r_{oa}}{R_o + R}} < 2.$$

Therefore, when matching both ports perfectly at low frequency, no more than 6 dB of negative feedback may be applied, so that the performance improvements associated with negative feedback are limited entirely by matching constraints.

To illustrate the tradeoff of gain for quality of match, we study the behavior of the scattering coefficients $s_{11}(j0)$, $s_{21}(j0)$, and $s_{22}(j0)$ with the variation of the normalized impedances $x \doteq r_{oa}/R$, $y \doteq R_f/R$, and $q \doteq R_o/R$. From (1), (3), (4), and (5), we obtain

$$s_{11}(j0) = \frac{1 - RY_{\text{in}}(j0)}{1 + RY_{\text{in}}(j0)} = \frac{y(x+q+1) + qx - (q+1)(k_o+1)}{y(x+q+1) + (q+2)x + (q+1)(k_o+1)} \quad (13)$$

$$s_{21}(j0) = 2A_f(j0) = \frac{-2(k_o y - x)}{(x+q+1)(y+1) + (k_o + x)(q+1)} \quad (14)$$

$$s_{22}(j0) = \frac{Z_{\text{out}}(j0) - R}{Z_{\text{out}}(j0) + R} = \frac{(q-1)(y+1+2x+k_o) + x(y+1)}{(q+1)(y+1+2x+k_o) + x(y+1)}. \quad (15)$$

Given q, we can compute loci of constant $s_{11}(j0)$, $s_{22}(j0)$, and $s_{22}(j0)$ in an $x-y$ plane. The results are:

1) for $s_{11}(j0) = c_{11}$, a constant, where $|c_{11}| < 1$:

$$\left[y + q + 1 - \left(\frac{1+c_{11}}{1-c_{11}}\right)\right](x+q+1) = (q+1)\left[\left(\frac{1+c_{11}}{1-c_{11}}\right)k_o + q + 1\right] \quad (16)$$

2) for $s_{22}(j0) = c_{22}$, a constant, where $|c_{22}| < 1$:

$$\left[y + 1 - 2\left(q - \frac{1+c_{22}}{1-c_{22}}\right)\right]\left[x - \frac{1+c_{22}}{1-c_{22}}\right] = (k_o+2)\left[q - \frac{1+c_{22}}{1-c_{22}}\right] \quad (17)$$

3) for $|s_{21}(j0)| = c_{21}$, a constant:

$$\left(x + q + 1 - \frac{2k_o}{c_{21}}\right)\left(y + 2 + q + \frac{2}{c_{21}}\right) = \left(2 + q + \frac{2}{c_{21}}\right)\left(1 + q - \frac{2k_o}{c_{21}}\right) - (q+1)(k_o+1). \quad (18)$$

For any q, the loci described by (16)–(18) are hyperbolas in the $x-y$ plane. Figs. 3–5 present these loci for a gain block with $k_o = 4$ and $q = 0$ when $R = 50\ \Omega$. By superimposing graphs of these loci, we may determine values for x, y, and q which effect the best tradeoff of gain and quality of match.

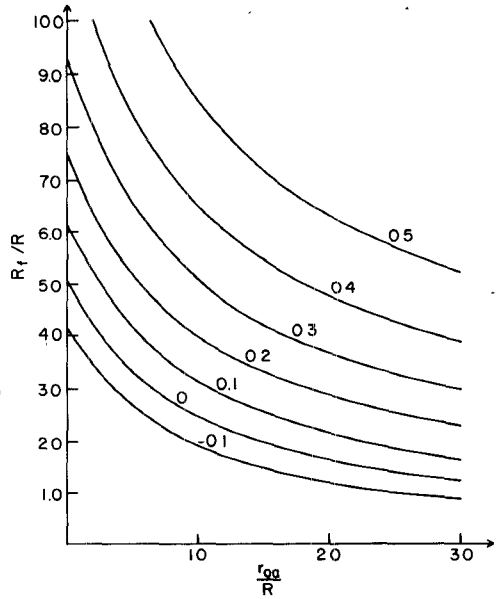

Fig. 3. Loci of constant $s_{11}(j0)$ for $k_o = 4$.

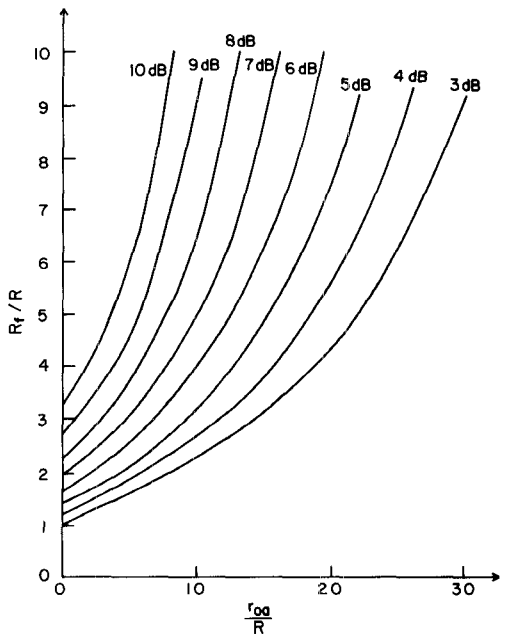

Fig. 4. Loci of constant $|s_{21}(j0)|$ for $k_o = 4$.

III. Broad-Band Amplifier Response

This section shows that broad-banding may be achieved by adjusting the impedance Z_1 (Fig. 1) and that satisfactory performance is obtained when Z_1 is a pure inductance. The analysis predicts a value for L_1 which serves as an excellent starting value for optimization by computer, and provides an estimate of the upper -3-dB frequency of the transducer voltage gain.

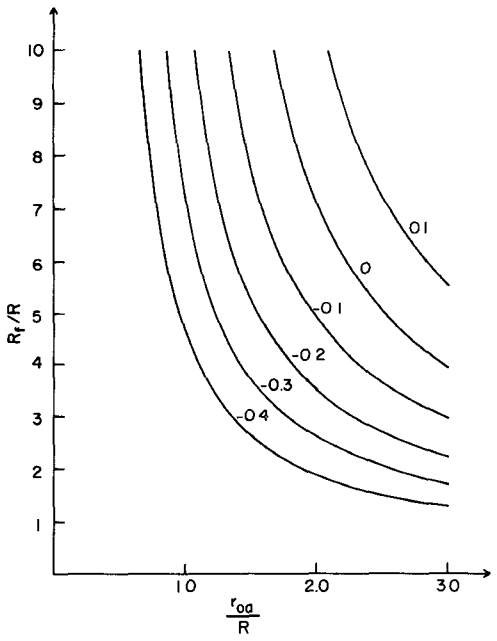

Fig. 5. Loci of constant $s_{22}(j0)$ for $k_o = 4$.

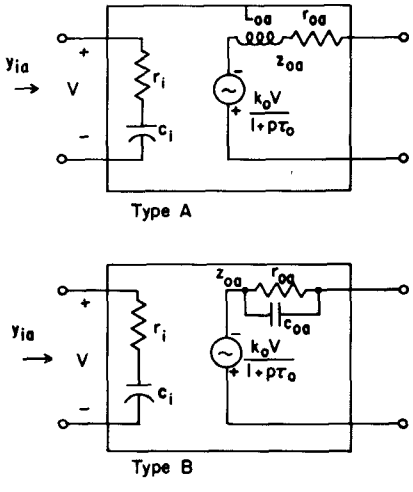

Fig. 6. Gain block models.

The gain block is represented by one of the unilateral models shown in Fig. 6. The model shown in Fig. 6(a) (type A, z_{oa} inductive) describes gain blocks with common-drain or common-collector output stages, and Fig. 6(b) (type B, z_{oa} capacitive) describes gain blocks with common-source or common-emitter output stages. Both types model the input port of the gain block by a resistance r_i in series with a capacitance c_i. By using optimization techniques, one can fit a type A or type B model to the measured or predicted s-parameters of the gain block.

To obtain estimates for the value of L_1 and the -3-dB frequency ω_m, the transducer voltage gain $A_f(p)$ in (3) is expanded and normalized to yield a rational function of the form

$$-\left[\frac{B_o A_f(p)}{M_o}\right] = \frac{1+\beta_1 p+\beta_2 p^2}{1+\xi_1 p+\xi_2 p^2+\xi_3 p^3+\xi_4 p^4} \tag{19}$$

TABLE I
RESULTS FOR TYPE A AND TYPE B GAIN BLOCKS

	TYPE A	TYPE B
z_{oa}	$r_{oa}+j\omega L_{oa}$	$r_{oa}/(1+j\omega r_{oa}c_{oa})$
τ_2	$L_{oa}M_o[1+G_f(R_o+R)]/(k_oR)$	$M_o c_{oa} r_{oa}(R_o+R)/(k_oR)$
α_1	$\omega_m[P(\tau_o+\tau_2)+Rc_i]/B_o$	$\omega_m[P(\tau_o+\tau_2-r_{oa}c_{oa})+Rc_i]/B_o$
α_2	$\omega_m^2[P(\tau_o\tau_2+L_1c_i)+Rc_i(\tau_o+\tau_2-\tau_i)]/B_o$	$\omega_m^2[P(\tau_o\tau_2+L_1c_i)+Rc_i(\tau_o+\tau_2-\tau_i)-c_{oa}r_{oa}\{P(\tau_o+\tau_2-c_{oa}r_{oa})+Rc_i\}]/B_o$
ω_m	$2\zeta B_o[P(\tau_o+\tau_2)+Rc_i]^{-1}$	$2\zeta B_o[P(\tau_o+\tau_2-c_{oa}r_{oa})+Rc_i]^{-1}$
L_1	$[B_o\omega_m^{-2}-P\tau_o\tau_2-Rc_i(\tau_o+\tau_2-\tau_i)]/(Pc_i)$	$[B_o\omega_m^{-2}-P\tau_o\tau_2-Rc_i(\tau_o+\tau_2-\tau_i)+c_{oa}r_{oa}\{P(\tau_o-c_{oa}r_{oa})+\tau_2+Rc_i\}]/(Pc_i)$

$P=1+RG_f$. $M_o=k_oR/[r_{oa}+(R_o+R)(1+r_{oa}G_f)]$. $B_o=1+RG_f+(R_o+R)G_fM_o$. $\tau_i=r_ic_i$. $\zeta=0.7$ for flat gain.

where

$$M_o \doteq \frac{k_oR}{r_{oa}+(R_o+R)(1+r_{oa}G_f)} \tag{20}$$

and

$$B_o \doteq 1+RG_f+(R_o+R)G_fM_o. \tag{21}$$

By expansion about $p=0$, (19) is approximated by an all-pole function

$$-\left[\frac{B_oA_f(p)}{M_o}\right] = \frac{1}{1+\alpha_1\left(\frac{p}{\omega_m}\right)+\alpha_2\left(\frac{p}{\omega_m}\right)^2+\cdots+\alpha_k\left(\frac{p}{\omega_m}\right)^k+\cdots} \tag{22}$$

which can be approximated over the passband by a second-order function:

$$-\left[\frac{B_oA_f(p)}{M_o}\right] \cong \frac{1}{1+2\zeta\left(\frac{p}{\omega_m}\right)+\left(\frac{p}{\omega_m}\right)^2}. \tag{23}$$

By choosing $\zeta=0.7$ in (23), we can calculate the value of inductance L_1 which yields flat broad-band gain, and a value for the -3-dB frequency ω_m. Results of this analysis for type A and type B gain blocks are summarized in Table I.

To complete the broad-band analysis, we examine the behavior of the functions $s_{11}(j\omega)$ and $s_{22}(j\omega)$. The function $s_{11}(j\omega)$ is weakly affected by $z_{oa}(j\omega)$, so that when investigating s_{11} we can assume that $z_{oa}(j\omega)\cong r_{oa}$. Expanded into partial fractions, the input admittance (4) becomes

$$Y_{\text{in}}(p) = \frac{p(c_i+C)+B}{1+p\tau_i+p^2L_1c_i}+\frac{1}{R_f+r_{oa}\|(R_o+R)}+\frac{A}{1+p\tau_o} \tag{24}$$

where

$$A=\frac{k_o\left[\frac{R_o+R}{r_{oa}+R_o+R}\right]\left[\frac{1}{R_f+r_{oa}\|(R_o+R)}\right]\tau_o(\tau_o-\tau_i)}{L_1c_i+\tau_o(\tau_o-\tau_i)} \tag{25}$$

$$B=k_o\left[\frac{R_o+R}{r_{oa}+R_o+R}\right]\left[\frac{1}{R_f+r_{oa}\|(R_o+R)}\right]-A \tag{26}$$

$$C=-B(\tau_o-\tau_i). \tag{27}$$

In general, $\tau_o>\tau_i$ so $A>0$, $B>0$, and $C>0$.

All terms in (24) are fixed by low-frequency design tradeoffs and flat-gain compensation, so the function

$$s_{11}(j\omega)=\frac{1-RY_{\text{in}}(j\omega)}{1+RY_{\text{in}}(j\omega)} \tag{28}$$

is also fixed. To evaluate the high-frequency performance of $s_{11}(j\omega)$, we can calculate $s_{11}(j\omega_m)$, $s_{11}(j\omega_o)$, and $s_{11}(j\omega_r)$, where ω_m is the -3-dB frequency predicted above, ω_o is the frequency where $\text{Im}[Y_{\text{in}}(j\omega)]=0$, and $\omega_r=1/\sqrt{L_1c_i}$.

At the frequency ω_o, one obtains

$$\text{Im}\left[Y_{\text{in}}(j\omega)\right] = 0 = -\frac{A\omega_o\tau_o}{1+\omega_o^2\tau_o^2}+\frac{\omega_o(c_i+C)\left[1-\frac{B\tau_i}{c_i+C}-\omega_o^2L_1c_i\right]}{\left(1-\omega_o^2L_1c_i\right)^2+\omega_o^2\tau_i^2}. \tag{29}$$

Rearranging (29), we obtain

$$\left(\omega_o^2L_1c_i\right)^2\left[1+\frac{\tau_o(c_i+C)}{AL_1c_i}\right]+\left(\omega_o^2L_1c_i\right)\left[\frac{\tau_i^2+\frac{B\tau_i\tau_o}{A}-\frac{\tau_o(c_i+C)}{A}}{L_1c_i}-2+\frac{(c_i+C)}{A\tau_o}\right]+1-\frac{c_i+C-B\tau_i}{A\tau_o}=0. \tag{30}$$

From (24) and (29), we can show that

$$Y_{\text{in}}(j\omega_o)=\frac{1}{R_f+z_{oa}\|(R_o+R)}+\frac{[(c_i+C)/\tau_o+B]\left[1-\omega_o^2L_1c_i\right]+\tau_i\left[\omega_o^2(c_i+C)-B/\tau_o\right]}{\left(1-\omega_o^2L_1c_i\right)^2+\omega_o^2\tau_i^2}. \tag{31}$$

The solution ω_o to (30) is substituted into (31) and s_{11} is calculated by (28).

The frequency ω_r generally lies near the passband edge. For small r_i, e.g., $r_i<R$, and for low high-frequency open-loop gain, we obtain

$$Y_{\text{in}}(j\omega_r)\to\frac{1}{r_i}+\frac{1}{R_f} \tag{32}$$

and therefore,

$$s_{11}(j\omega_r)\to\frac{1-\frac{R}{r_i}-\frac{R}{R_f}}{1+\frac{R}{r_i}-\frac{R}{R_f}}. \tag{33}$$

This relationship demonstrates that high-frequency s_{11} is strongly dependent on the value of r_i. When r_i is not approximately equal to R, it may be necessary to add an input-matching network in order to obtain acceptable high-frequency matching. Finally, we note that the frequencies ω_m, ω_o, and ω_r are usually close to one another, so a computation of s_{11} at one of these frequencies is sufficient.

To estimate the high-frequency performance of s_{22}, it is best to simply calculate

$$Y_o(j\omega_m)\cong\frac{1}{z_{oa}(j\omega_m)}+G_f\left\{1-\left[1+\frac{R_o+R}{z_{oa}(j\omega_m)}\right]A_o(j\omega_m)\right\} \tag{34}$$

and

$$s_{22}(j\omega_m)=\frac{1-(R-R_o)Y_o(j\omega_m)}{1+(R-R_o)Y_o(j\omega_m)}. \tag{35}$$

IV. Design Procedure

A. Gain Block Synthesis and Modeling

In this step a gain block composed of FET's or BJT's is designed, and a small-signal broad-band model of the form shown in Fig. 6(a) (type A) or Fig. 6(b) (type B) is derived. Biasing circuit details are considered as part of the gain block design. In synthesizing small-signal models of the gain block, the authors have characterized the individual devices which compose the gain block by measured s-parameter data or by the equivalent circuit shown in Fig. 8. Then, we have used a general circuit analysis program to compute the scattering parameters of the gain block and have used an optimization program to fit the appropriate type A or type B gain model to these gain block s-parameters.

B. Low-Frequency Design

Equations (13)–(15) and/or the loci described by (16)–(18) are used to choose values for R_f and R_o which lead to an acceptable tradeoff of gain and port matches. If perfect low-frequency port matches are required, (10) and (11) may be employed, but this choice may lead to unacceptably low gain. To improve the low-frequency output match, the gain block output impedance z_{oa} may be

adjusted by adding series resistance or by scaling the active devices.

C. Broad-banding

The value of inductance L_1 and the predicted -3-dB bandwidth are calculated using the design equations listed in Table I. The scattering parameters s_{11} and s_{22} are computed at high frequency, as described in Section III.

D. Optimization of the Basic Amplifier

The values of L_1, R_f, and R_o and of any variable elements of the gain block are adjusted by the minimization of a suitable function, e.g.,

$$\sum_{k=0}^{K}\left[w_{11}|s_{11}(jk\Delta\omega)|^2+w_{22}|s_{22}(jk\Delta\omega)|^2 + w_{21}\left(|s_{21}(jk\Delta\omega)|_{\mathrm{dB}}-T\right)^2\right] \quad (36)$$

where

$$\Delta\omega=\frac{\omega_m}{K}$$

and T is the target gain in dB. Here, the value of ω_m is given in Table I and the w_{ij} are positive real weights. This optimization will indicate whether the bandwidth and/or the gain specifications may be tightened. If the matching performance is not acceptable, input and/or output matching networks may be added. Optimization of these networks is interactive because the feedback amplifier is not unilateral.

If a monolithic realization is desired, the inductors may be replaced by high-impedance lines and a final optimization step may be carried out.

V. Design Examples

Example 1: In this example, the gain block consists of the parallel connection of experimental 0.8×300 μm GaAs MESFET's shown in Fig. 7. The system impedance is $R=50\ \Omega$.

By optimizing the fit of the small-signal model (see [15], [16]) to (all four) measured s-parameters, this MESFET may be represented by a small-signal model (Fig. 8) consisting of the elements $r_{gg'}=18.8\ \Omega$, $r_g=3$, $C_g=0.265$ pF, $r_{ss'}=2.4$, $c_{gd}=0.05$, $c_{ds}=0.0563$, $r_{ds}=216$, $r_{dd'}=3$, $g_m=37.5$ mS, and $\tau=2$ ps. Since the gain block output impedance z_{oa} is capacitive, the gain block is type B. By curve-fitting the type B model to calculated gain block s-parameters, we obtain $r_i=19.2\ \Omega$, $c_i=0.928$, $r_{oa}=60.2$, $c_2=0.58$, $k_o=4.047$, and $\tau_o=35.4$ ps.

Figs. 3–5 show that with $k_o=4$, close to the value calculated above, we obtain $|s_{21}|\cong 7$ dB with $R_o/R=0$ and $R_f/R=6$. These ratios are chosen as the initial values for the design. Using (13) and (15), we calculate $s_{11}(j0)=0.4$, $s_{22}(j0)=-0.26$, and from Table I we compute $\tau_2=14.6$ ps, $M_o=1.684$, $B_o=1.447$, $\omega_m=3.177\cdot10^{10}$ (5.05 GHz), and $L_1=1.37$ nH. From (30), we obtain $\omega_o=2.66\cdot10^{10}$ (4.23 GHz); from (30), (31), and (28), we obtain $s_{11}(j\omega_o)=-0.456$; and from (34), (1), and (35), we obtain $s_{22}(j\omega_m)=0.46$. These results predict only fair high-frequency port matches.

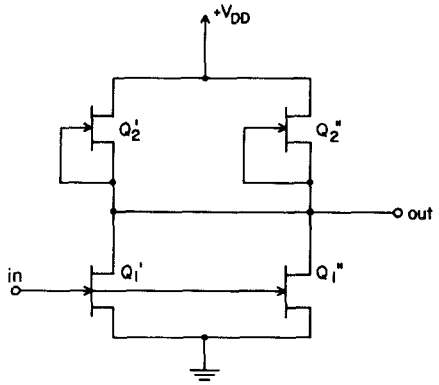

Fig. 7. Gain block, design example 1.

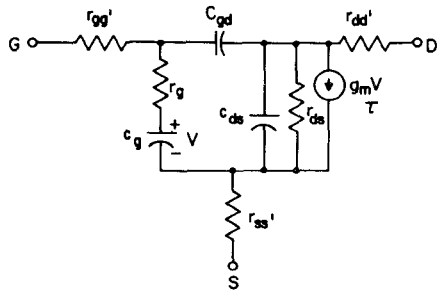

Fig. 8. GaAs MESFET small-signal model.

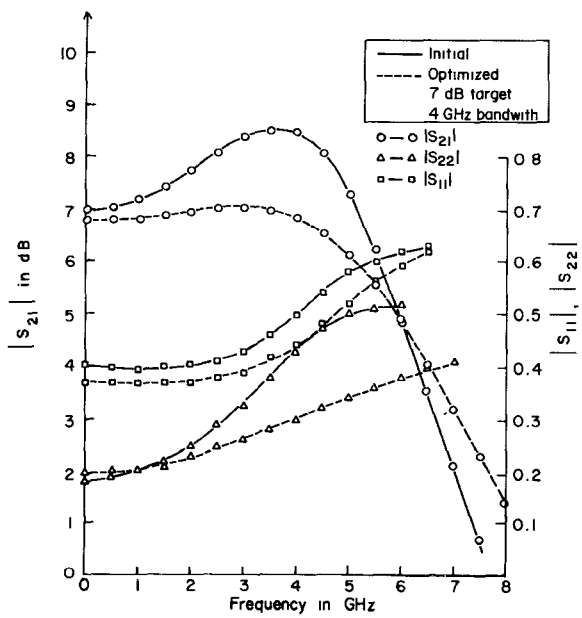

Fig. 9. Response curves, design example 1.

Fig. 9 shows the initial response and the response optimized via (36) over [0, 4] GHz using the target gain $|s_{11}|=7$ dB, with $w_{11}=0.5$, $w_{21}=1.0$, and $w_{22}=0.5$. The final element values are $L_1=1.18$ nH and $R_f=283\ \Omega$. To

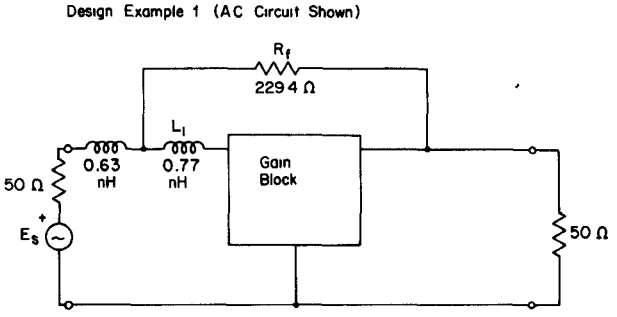

Fig. 10. Optimized 6-dB, 4-GHz amplifier.

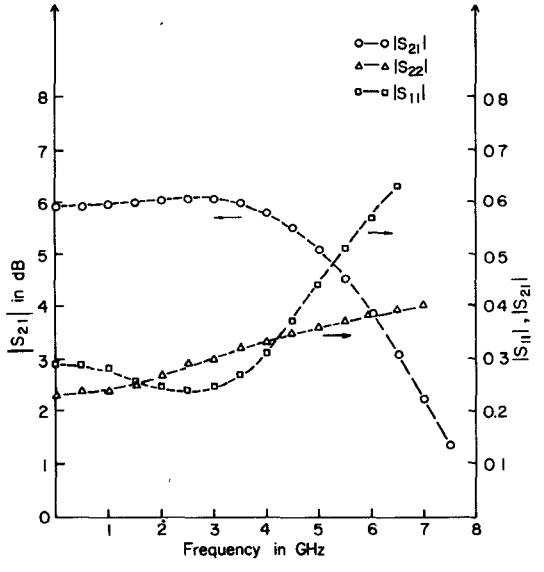

Fig. 11. Response curves, design example 1.

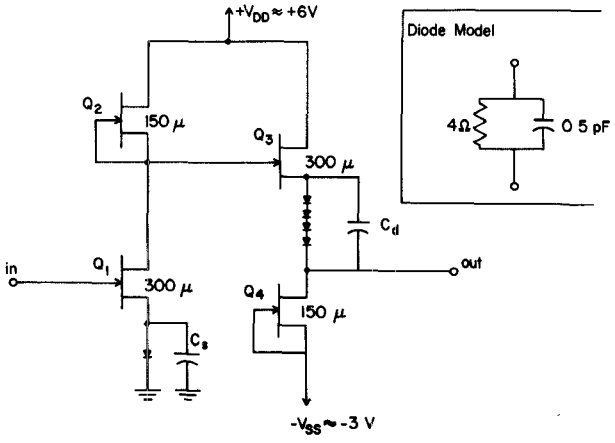

Fig. 12. Gain block, design example 2.

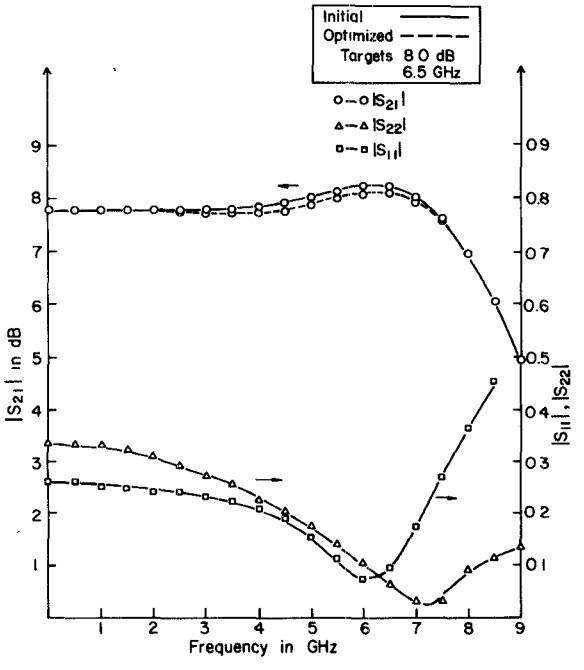

Fig. 13. Response curves, design example 2.

improve the behavior of the port matches, the gain target is reduced to 6 dB and a simple lossless input port matching network is synthesized. The resulting circuit is shown in Fig. 10 and the optimized response is presented Fig. 11. The predicted gain is $|s_{21}| = 5.8 \pm 0.3$ dB over [0,4.5] GHz, and the predicted -3-dB frequency is approximately 6.7 GHz.

Example 2: In this example, the gain block consists of a circuit similar to the one proposed by Hornbuckle [18] (Fig. 12), where transistors Q_1 and Q_3 are identical 0.8×300 μm MESFET's and Q_2 and Q_4 are 0.8×150 μm MESFET's. The element values in the small-signal model of the 150-μm device are $r_{gg'} = 8$ Ω, $r_g = 3.33$, $c_g = 0.105$ pF, $c_{gd} = 0.0168$, $g_m = 15.75$ mS, $c_{ds} = 0.024$, $r_{ds} = 524$, $r_{ss'} = 4.67$, $r_{dd'} = 6.4$, and $\tau = 2$ ps. The capacitance C_d is adjusted to make z_{oa} nearly resistive across the passband, and the bypass capacitance C_g is chosen to be 4.5 pF. The system impedance is $R = 50$ Ω. For this gain block, $r_i = 36.6$ Ω, $c_i = 0.323$ pF, $\tau_i = 11.9$ ps, $\tau_o = 35.4$ ps, $k_o = 4.32$, and $z_{oa} \cong r_{oa} = 46.8$. For $R_o/R = 0$ and $R_f/R = 5$, we obtain $s_{11}(j0) = 0.258$, $|s_{21}(j0)| = 7.78$ dB, $s_{22}(j0) = -0.369$, $M_o = 2.034$, and $B_o = 1.607$. From Table I, type A, with $L_{oa} = 0$, we obtain $\omega_m = 3.84 \cdot 10^{10}$ (6.11 GHz) and $L_1 =$ 1.83 nH. From (24)–(28), (30), and (31), we obtain $\omega_o = 3.84 \cdot 10^{10}$ (5.76 GHz) and $s_{11}(j\omega_o) = 0.12$, an excellent high-frequency match. Through (35), we obtain $|s_{22}(j\omega_m)| = 0.033$.

Initial and optimized response curves for the basic feedback amplifier are presented in Fig. 13. The bandwidth and gain targets are, respectively, 7.5 GHz and 8 dB. In this example, the initial estimate for L_1 is close to the optimum value, so the optimization yields little improvement except for a slight flattening of gain. The optimized elements are $L_1 = 1.765$ nH, $C_d = 2.53$ pF, and $R_f = 267$ Ω. The predicted gain is 7.98 ± 0.18 dB from dc to 7.2 GHz, and the predicted -3-dB frequency is 9 GHz.

To obtain a circuit suitable for MMIC realization, L_1 is replaced by a high-impedance transmission line, and overall optimization is carried out. The circuit and its performance are described by Figs. 14 and 15. The predicted

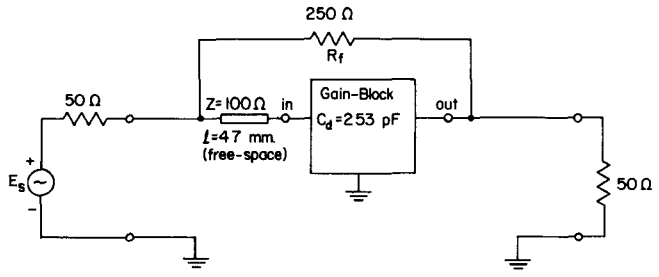

Fig. 14. Optimized distributed realization.

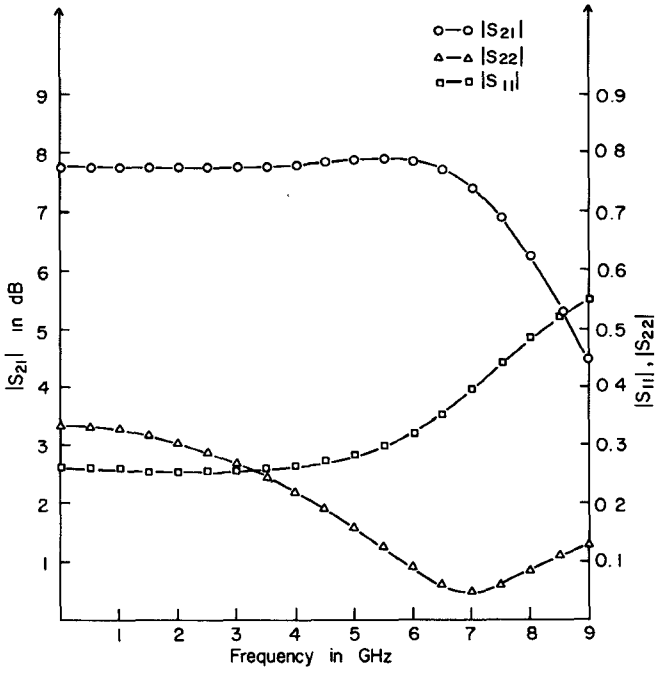

Fig. 15. Response curves, optimized distributed realization.

gain is 7.8 ± 0.1 dB from dc to 6.5 GHz, and the predicted -3-dB frequency is 8.7 GHz.

VI. Conclusions

We have analyzed the low- and high-frequency properties of a small-signal amplifier which consists of a generalized gain block, resistive shunt feedback, and broadbanding circuitry. The synthesis procedure presented in the paper yields circuit element values and provides estimates of gain and bandwidth. When these element values are used as starting values in an optimization step, convergence is rapid.

The basic amplifier has been modified by adding matching networks and by substituting distributed elements for lumped elements. In an example, we have designed a direct-coupled feedback amplifier, suitable for MMIC realization, for which a 7.8 ± 0.1 dB gain from dc to 7.2 GHz and a -3-dB bandwidth of 9 GHz are predicted.

Acknowledgment

The authors acknowledge the assistance of J. He, of the Hebei Semiconductor Research Institute, in formulating design example 2. They also acknowledge the assistance of Dr. W. Peterson for providing device descriptions and for laying out an amplifier prototype.

References

[1] K. B. Niclas, "Multi-octave performance of single-ended microwave solid-state amplifiers," *IEEE Trans. Microwave Theory Tech.*, vol. MTT-32, pp. 896–908, Aug. 1984.

[2] K. B. Niclas, "The exact noise figure of amplifiers with parallel feedback and lossy matching circuits," *IEEE Trans. Microwave Theory Tech.*, vol. MTT-30, pp. 832–835, May 1982.

[3] K. Honjo, Y. Takayama, "GaAs ultrabroad-band amplifiers for Gbit/s data rate systems," *IEEE Trans. Microwave Theory Tech.*, vol. MTT-29, July 1981.

[4] K. Honjo, T. Sugiura, T. Tsuji, and T. Ozawa, "Low-noise, low-power-dissipation GaAs monolithic broad-band amplifiers," *IEEE Trans. Microwave Theory Tech.*, vol. MTT-31, pp. 412–417, May 1983.

[5] C. E. Weitzel, and D. Scheitlin, "Single-stage GaAs monolithic feedback amplifiers," *IEEE Trans. Microwave Theory Tech.*, vol. MTT-33, pp. 1244–1249, Nov. 1985.

[6] E. Ulrich, "Use feedback to slash wideband VSWR," *Microwaves*, pp. 66–70, Oct. 1978.

[7] S. Moghe, H. Sun, T. Andrade, C. Huang, and R. Goyal, "A monolithic direct-coupled GaAs IC amplifier with 12-GHz bandwidth," *IEEE Trans. Microwave Theory Tech.*, vol. MTT-32, pp. 1698–1703, Dec. 1984.

[8] W. Peterson, A. K. Gupta, and D. R. Decker, "A monolithic GaAs dc to 2 GHz feedback amplifier," *IEEE Trans. Microwave Theory Tech.*, vol. MTT-31, pp. 27–29, Jan. 1983.

[9] P. Terzian, D. Clark, and R. Waugh, "Broad-band GaAs monolithic amplifier using negative feedback," *IEEE Trans. Microwave Theory Tech.*, vol. MTT-30, pp. 2017–2020, Nov. 1982.

[10] A. M. Pavio, "A network modeling and design method for a 2–18-GHz feedback amplifier," *IEEE Trans. Microwave Theory Tech.*, vol. MTT-30, pp. 2212–2216, Dec. 1982.

[11] J. Beall, S. R. Nelson, and R. Williams, "Design and process sensitivity of a two-stage 6–18-GHz monolithic feedback amplifier," *IEEE Trans. Microwave Theory Tech.*, vol. MTT-33, pp. 1567–1571, Dec. 1985.

[12] J. Tajima, Y. Yamao, T. Sugeta, and M. Hirayama, "GaAs monolithic low-power amplifiers with *RC* parallel feedback," *IEEE Trans. Microwave Theory Tech.*, vol. MTT-32, pp. 542–544, May 1984.

[13] K. B. Niclas, W. T. Wilser, R. B. Gold, and W. R. Hitchins, "The matched feedback amplifier: Ultrawide-band microwave amplification with GaAs MESFET's," *IEEE Trans. Microwave Theory Tech.*, vol. MTT-28, pp. 285–294, Apr. 1980.

[14] J. A. Archer, H. P. Weidlich, E. Pettenpaul, F. Petz, and J. Huber, "A GaAs monolithic low-noise broad-band amplifier," *IEEE J. Solid-State Circuits*, vol. SC-16, no. 6, pp. 648–652, Dec. 1981.

[15] F. Perez and V. Ortega, "A 0.15–12-GHz matched feedback amplifier using commercially available FET's," *IEEE Trans. Microwave Theory Tech.*, vol. MTT-30, pp. 1289–1290, Aug. 1982.

[16] H. Kondoh, "Accurate FET modeling from measured *s*-parameters," in *1986 IEEE MTT Symp. Dig.*, pp. 377–380.

[17] R. A. Minasian, "Simplified GaAs M.E.S.F.E.T. model to 10 GHz," *Electron. Lett.*, vol. 13, no. 18, pp. 549–551, Sept. 1977.

[18] D. Hornbuckle, "GaAs direct-coupled amplifiers," in *IEEE MTT Symp. Dig.*, 1980, pp. 387–389.

David J. Ahlgren (S'73–M'75) was born in New Britain, CT, on December 22, 1942. He received the B.S. degree in engineering (cum laude) from Trinity College, Hartford, CT, the M.S. degree in electrical engineering from Tulane University, New Orleans, LA, and the Ph.D. degree in electrical engineering from the University of Michigan, Ann Arbor. While pursuing his graduate studies, he was supported by a NIH research

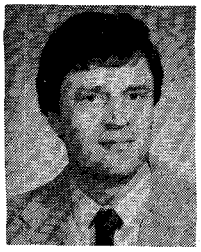

assistantship and by NASA and NSF traineeships.

Since 1973, he has been on the faculty at Trinity College, where he is currently Associate Professor of Engineering and Computer Science. In 1981, he was Visiting Associate Professor of Electrical Engineering at Cornell University. His interests include the investigation of gain–bandwidth limits in broad-band amplifiers, the design of monolithic microwave feedback amplifiers, system modeling and simulation, and the design of portable microprocessor-based instruments for evaluating performance in sports. He has been active in the Alfred P. Sloan Foundation New Liberal Arts Program, which supports the study of technology in liberal arts colleges.

Dr. Ahlgren is a member of Sigma Xi and Delta Phi Alpha and has been an officer of the Connecticut Section of IEEE.

✠

Walter H. Ku (S'56–M'62) received the B.S. degree (with honors) from the Moore School of Electrical Engineering of the University of Pennsylvania, Philadelphia, PA, and the M.S. and Ph.D. degrees in electrical engineering from the Polytechnic Institute of Brooklyn, NY. From 1957 to 1960, he held a Research Fellowship at the Polytechnic Institute of Brooklyn.

From 1960 to 1962, he was on the research staff of the Microwave Research Institute (MRI) of the Polytechnic Institute of Brooklyn. From 1962 to 1969, he was with the Applied Research Laboratory of Sylvania Electronic Systems as an Engineering Specialist, a Senior Engineering Specialist, and a Senior Scientist. He joined the faculty of the School of Electrical Engineering of Cornell University in 1969 and was Professor of Electrical Engineering. In 1973–1974, he was on leave from Cornell and was a visiting Associate Professor at the Department of Electrical Engineering and Computer Science of the University of California, Berkeley. For the 1977 academic year, he was on sabbatical leave from Cornell and was the first occupant of the Naval Electronic Systems Command (NAVELEX) Research Chair Professorship at the Naval Postgraduate School, Monterey, CA. For the 1983–1984 academic year, he was a Distinguished Visiting Professor at the Department of Electrical Engineering and Computer Science of the University of California, San Diego, La Jolla. He joined the faculty of UCSD as Professor of Electrical Engineering and Computer Sciences in September 1985. He has served over the years as a consultant to Air Force RADC, NRL, NAVELEX, AFCS, DARPA, and industrial laboratories. He is presently a Consultant to the Department of Defense. His current research interests are in the area of design and fabrication of submicrometer gate-length MOS and GaAs FET's, HEMT's, and GaAlAs/GaAs heterojunction bipolar transistors, monolithic microwave and millimeter devices and IC's, phased array modules and sampled analog and digital signal processing techniques, and VLSI/VHSIC chip architectures and gigabit logic.

Dr. Ku is a member of Eta Kappa Nu, Tau Beta Pi, Sigma Tau, Phi Tau Phi, and Sigma Xi. He was a Faculty member of the National Research and Resource Facility for Submicron Structures (NRRFSS) and was a Member of the Executive Committee of the new Semiconductor Research Corporation (SRC) Center of Excellence on Microstructure and Technology, established at Cornell University. He was an Associate Editor of the IEEE TRANSACTIONS ON CIRCUITS AND SYSTEMS and he was Co-Chairman of the Technical Committee on Optical, Microwave and Acoustical Circuits of the IEEE Circuits and Systems Society and a Co-Chairman of the Technical Committee on Microwave Computer-Aided Design of the IEEE Microwave Theory and Techniques Society. He is currently an Associate Editor of the *Journal of the Franklin Institute* and a member of the Editorial Board of the IEEE TRANSACTIONS ON MICROWAVE THEORY AND TECHNIQUES. He is also a member of the IEEE Defense R&D Committee.